RAPID COMMUNICATIONS

PHYSICAL REVIEW B **81**, 161411(R) (2010)

Scanning probe energy loss spectroscopy with microfabricated coaxial tips

M. Y. Song,[1] J. J. Lawton,[1] A. P. G. Robinson,[1,2] and R. E. Palmer[1,*]

[1]*Nanoscale Physics Research Laboratory, School of Physics and Astronomy, University of Birmingham, Edgbaston, Birmingham B15 2TT, United Kingdom*

[2]*School of Chemical Engineering, University of Birmingham, Edgbaston, Birmingham B15 2TT, United Kingdom*

(Received 8 February 2010; published 26 April 2010)

We report scanning probe energy loss spectroscopy (SPELS) measurements of a graphite surface taken with microfabricated coaxial tips. The SPELS spectra of graphite obtained with a grounded coaxial tip show the π and σ plasmon peaks and intense secondary electron emission (SEE) peaks. In comparison, spectra taken with a simple Au cathode tip also showed the π and σ plasmon peaks but much weaker SEE peaks. The enhanced collection of secondary electrons enables the unoccupied band structure of the surface (i.e., above E_{vac}) to be explored.

DOI: 10.1103/PhysRevB.81.161411 PACS number(s): 07.79.Cz, 79.20.Uv, 73.20.Mf, 79.20.Hx

Since Binnig and Rohrer invented the scanning tunnelling microscope (STM) in the early 1980s, STM has become a powerful tool to characterize a surface in real space with atomic-scale spatial resolution.[1] However, STM is limited in its capacity to provide information on the chemical nature of the atoms it images. Several groups are developing STM-based techniques to obtain additional information, e.g., scanning probe energy loss spectroscopy (SPELS),[2–9] field emission STM,[10–15] and STM Auger electron energy spectroscopy[16,17] as well as STM low-energy electron diffraction.[18–21] The tips in these modified instruments typically operate in field emission mode, creating a local electron flux above the vacuum level, E_{vac}. Electrons scattered from the surface can then be analyzed to provide local information about the elemental composition or structure. A spatial resolution of ~10 nm has been reported in SPELS.[6] However, the electric field applied between tip and surface to facilitate the field emission of electrons also has negative side effects: it distorts the trajectories of the backscattered electrons and reduces the signal detected.[4] Therefore shielding of the tip has obvious attractions. Electrochemically etched tungsten tips mounted within a chromium-coated borosilicate tube[16,20] and a coaxial gold-plated macroscopic tip holder have been explored previously.[12] However, these devices only shield the electric field macroscopically. Ideally the field should be excluded to within a few microns of the tip-surface junction.

Here we report SPELS measurements using a microfabricated coaxial tip. A schematic of the measurement geometry is shown in Fig. 1(a). The multilayer coaxial tip consists of $Si/Au/HfO_2/Au$ layers; the outer Au and HfO_2 layers are stripped from the apex of the tip, Fig. 1(b). The inner and outer Au layers are used as the emitting and the screening layers, respectively. The multistep microfabrication process is described in detail elsewhere.[22] The benefit of a microfabricated coaxial tip compared with, for instance, a glass-covered electrochemically etched tungsten tip is fine control of the coaxial structure. A microfabricated tip with an Au-emitting layer but no coaxial screening layer, Fig. 1(c), was also fabricated for comparative experiments and is termed the "Au cathode tip."

The SPELS instrument itself is based on an Omicron STM 1 head combined with a VG 100 AX hemispherical electron energy analyzer mounted parallel to the surface plane, in an ultrahigh vacuum chamber with a base pressure of 5×10^{-10} mbar. The hemispherical analyzer incorporates an electrostatic entrance lens that transfers electrons from the sample to the entrance slit of the analyzer sectors, Fig. 1(a). The way the electrostatic lens is tuned determines the angular acceptance of the hemispherical analyzer.[23] The distance between sample and analyzer is 40 mm. Note that the count rates in the spectra shown in Fig. 2 below are normalized to the measured current incident on the surface and thus measure the efficiency of the combined processes of electron scattering, escape, and detection.

SPELS spectra were collected from the graphite basal plane using the coaxial tips and one of two different lens

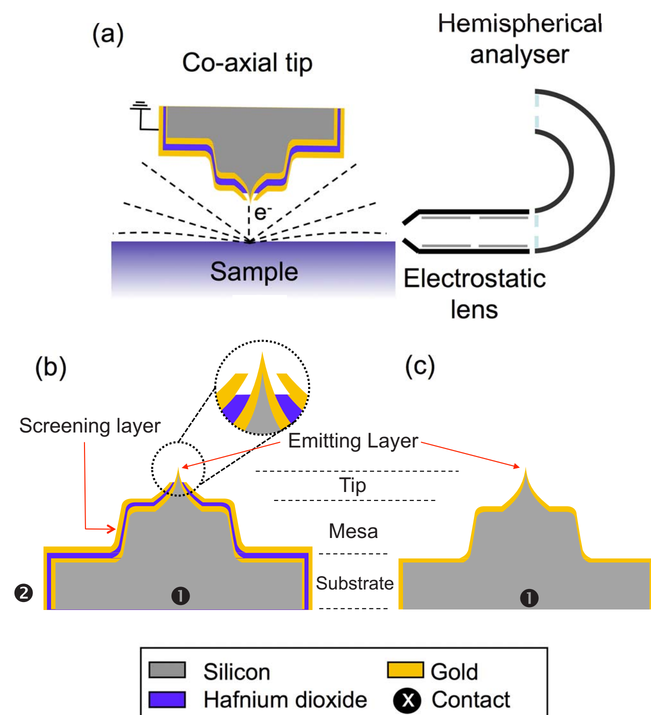

FIG. 1. (Color online) Schematics of (a) the SPELS geometry employed in this work, (b) the coaxial tip, and (c) the Au cathode tip.

 ©2010 The American Physical Society

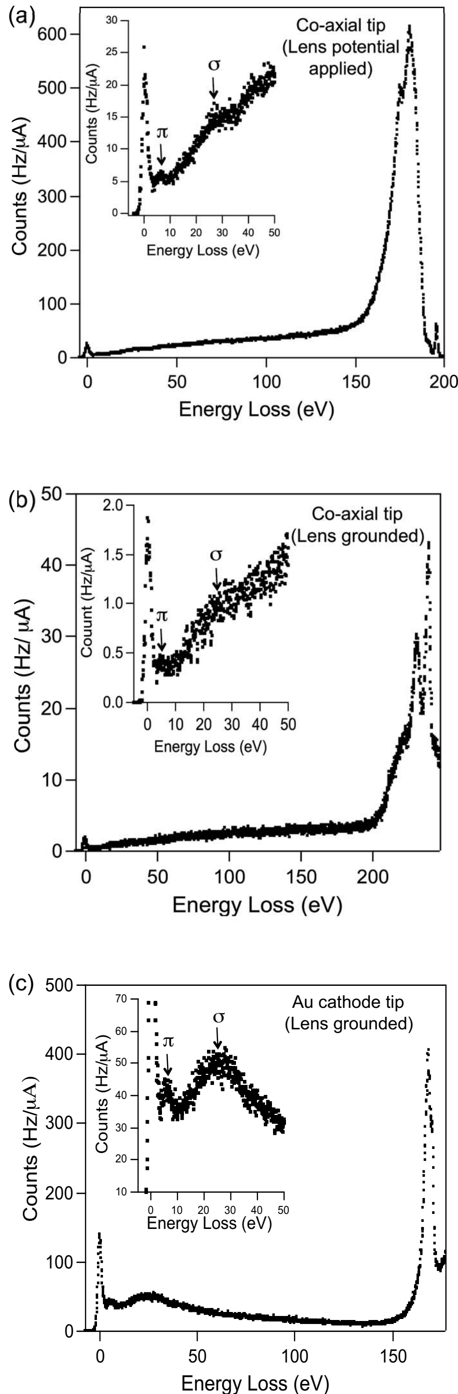

FIG. 2. SPELS spectra of graphite taken with (a) coaxial tip (tip bias voltage −200 V, working distance 250 nm, lens potential applied), (b) coaxial tip (tip bias voltage −250 V, working distance 250 nm, lens grounded), and (c) Au cathode tip (tip bias voltage −180 V, working distance 638 nm, lens grounded).

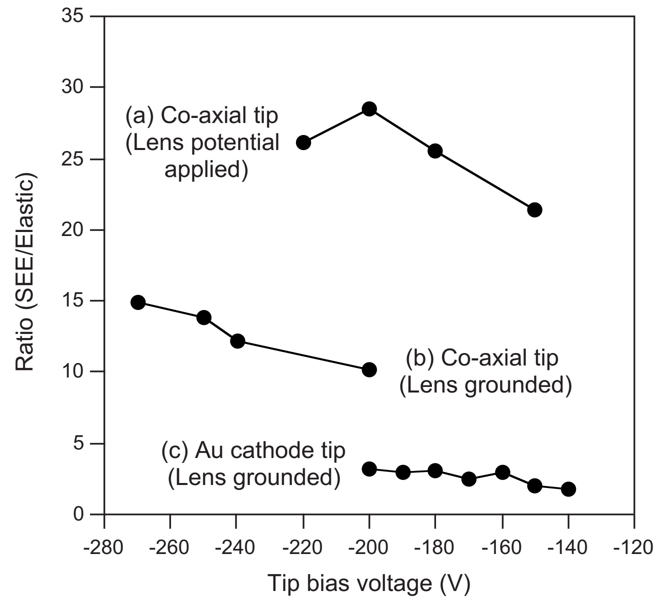

FIG. 3. The ratio between SEE peak intensities and elastic peak intensities as a function of the tip bias voltage for (a) coaxial tip (lens potential applied), (b) coaxial tip (lens grounded), and (c) Au cathode tip (lens grounded).

configurations. Figure 2(a) shows a spectrum collected with a positive lens potential applied (to focus the incoming electrons onto the entrance slit); for Fig. 2(b) this lens is grounded. In Fig. 2(c), for comparison, a spectrum of graphite is shown that was again taken with the lens grounded but using the Au cathode tip.

From the SPELS spectra taken with the coaxial tips in Figs. 2(a) and 2(b), it can be seen that the familiar π ($\sim$6 eV) and σ ($\sim$26 eV) graphite plasmons have comparatively weak intensity, but the secondary electrons peaks are very prominent, exceeding the elastic peak intensity. The same coaxial tip was used to take the spectra in both Figs. 2(a) and 2(b); the only difference is the electrostatic lens bias, which sets the angular acceptance, as discussed. In Fig. 2(a), the positive potential applied to the lens increases the angular range of electrons collected, and the result is a broadening of the (very intense) SEE peaks. In Fig. 2(b), the lens is grounded and only electrons within a narrow angular range are detected. Two intense SEE peaks are clearly observed under these conditions. The spectrum in Fig. 2(c) taken with the Au cathode tip (lens grounded, thus narrow angular acceptance) shows the elastic peak, well-developed π (6 eV) and σ (26 eV) plasmons and secondary electron peak, and is similar to that obtained with an electrochemically etched tungsten tip.[7]

The principal feature of the spectra taken with the coaxial tips is thus the enhancement of the SEE peak intensities. Figure 3 plots the ratio between SEE peak and elastic peak intensities as function of the tip bias voltage for the tips in Fig. 2. The ratio between the SEE and elastic peaks in Figs. 3(a)–3(c) are 28.5, 10.1, and 3.2, respectively, at the tip bias voltage of −200 V. When a potential is applied to the lens, Fig. 3(a), the ratio [secondary electron emission (SEE)/elastic peak] is found to be 2.8 times higher than when the lens is grounded, Fig. 3(b), consistent with the increased angular acceptance. The coaxial tip shows a threefold enhancement in the ratio (SEE/elastic peak) compared with the Au cathode tip under the same conditions (lens grounded).

In Fig. 4 the SEE peaks of graphite from Fig. 2 are replotted against kinetic energy in the range 0–50 eV. For convenience the spectra are normalized with respect to each

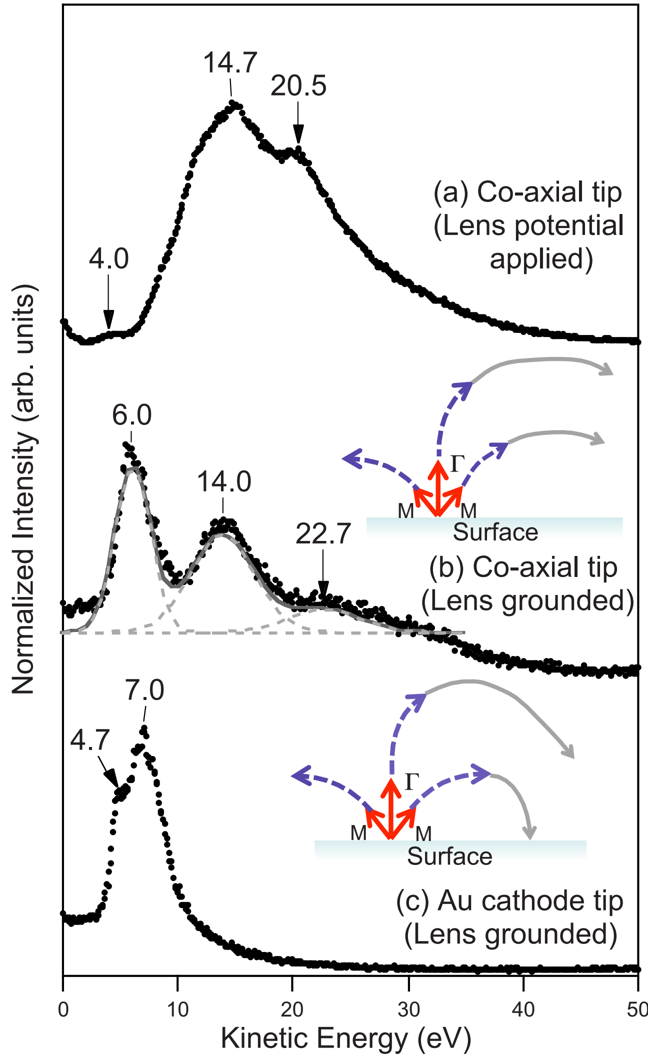

FIG. 4. (Color online) SEE spectra from SPELS of graphite taken with (a) coaxial tip (lens potential applied), (b) coaxial tip (lens grounded), and (c) Au cathode tip (lens grounded). (b) shows the Gaussian fitting used to determine peak positions. The insets to (b) and (c) are schematics of the secondary electron trajectories.

other, using the most intense peak in each spectrum. The SEE spectra obtained with the coaxial tip each show several peaks, Fig. 4(a) (lens potential applied) and Fig. 4(b) (lens grounded). In Fig. 4(a) the peaks are at 4.0, 14.7, and 20.5 eV while in Fig. 4(b) three peaks at 6.0, 14.0, and 22.7 eV are clearly seen. For the Au cathode tip, Fig. 4(c), only a SEE peak at 7.0 eV and a small shoulder at 4.7 eV are observed. Thus the coaxial screening of the tip field not only increases the overall secondary electron signal but also exposes new SEE peaks. Table I summarizes the assignment of the peaks observed, based on previous experimental reports[7,9] and especially the critical points in the theoretically calculated unoccupied band structure of graphite.[24,25] Values are given relative to the Fermi level. The secondary electron peaks at particular kinetic energies can thus be assigned to particular points in the unoccupied band structure of the surface. Most SEE features observed can be associated with electrons coming from the zone center (Γ point) of the Brillouin zone. It seems that secondary electrons from the Γ point, which are emitted perpendicular to the surface can be deflected by the tip electric field so that the analyzer (located parallel to the surface) can still detect them [see schematic in Fig. 4(c)]. So, for example, the SEE peaks measured with the Au cathode tip, Fig. 2(c), at 4.7 and 7.0 eV, both come from the Γ point in the band structure. However, some SEE features appear to be associated with the edge of the Brillouin zone. For example, the peak at 14.7/14.0 eV in Figs. 4(a) and 4(b), both obtained with the coaxial tip, seems to be associated with an unoccupied state at the *M* point.

In order to understand better which peaks are observed in the SEE spectra, it is helpful to consider, at least qualitatively, the trajectories of the secondary electrons. The electrons field emitted from the tip are incident on the surface, following the electric field lines in the tip-surface junction. These incident electrons are backscattered, both elastically and inelastically, and secondary electrons are also generated. The secondary electrons are emitted at different angles with respect to the surface depending on which symmetry point in the Brillouin zone they originate from (Γ point or *M* point in this case). Once they leave the surface they will experience

TABLE I. Comparison between the energies of peaks observed in the SEE spectra and critical points in the unoccupied band structure.

Band assignment	Experimental (eV, in Fig. 4)	Theory (eV)
Coaxial tip		
$\sigma(\Gamma_3^+)$ (Ref. 25)/$\pi(M_2^-)$ (Ref. 25)	4.0	4.0 (Γ, M) (Ref. 25)
$\pi(\Gamma_3^+)$ (Refs. 24 and 25)/$\sigma(M_5^+, M_6^-)$ (Ref. 25)	6.0	5.8 (Γ) (Ref. 25)/6.3 (M) (Ref. 25)
$\sigma(M_3^-, M_4^+)$ (Ref. 24)	14.0	14.0 (M) (Ref. 24)
	14.7	
$\sigma(\Gamma_1^+)$ (Ref. 24)/$\pi(M_2^+)$ (Ref. 24)	20.5	20.6 (Γ) (Ref. 24)/20.5 (M) (Ref. 24)
$\pi(\Gamma_2^-)$ (Ref. 24)/$\pi(M_4^-)$ (Ref. 24)	22.7	22.0 (Γ) (Ref. 24)/22.8 (M) (Ref. 24)
Au cathode tip		
$\sigma(\Gamma_5^+, \Gamma_6^-)$ (Ref. 25)	4.7	4.8 (Γ) (Ref. 25)
$\pi(\Gamma_3^+)$ (Ref. 24)	7.0	7.0 (Γ) (Ref. 24)

the tip-surface electric field. When an unshielded tip is used, the range of this field is unconstrained. The trajectories of secondary electrons from, say the M point, (which are emitted at a shallow angle to the surface) are thus likely to be bent back into the surface without reaching the analyzer. By contrast, secondary electrons from the Γ point (emitted normal to the surface) may be bent into the analyzer, fixed parallel to the surface [Fig. 4(c)], and thus detected more efficiently than if there were no tip-surface field. However, when a shielded coaxial tip is used, the electric field is confined to the immediate proximity of the tip-surface junction. Secondary electrons are thus able to escape from the tip region with less distortion of their trajectories; hence the increased signal of electrons from the M point of the Brillouin zone [Fig. 4(b)]. This effect also accounts for the higher SEE/elastic ratio shown [in Figs. 3(a) and 3(b)] by the screened tip compared with the unshielded tip [Fig. 3(c)]. The key result is then the enhancement of (local) secondary electron features away from the zone center when a screened coaxial tip is employed in SPELS. In future, angular-resolved measurements with the coaxial tips would be particularly instructive. Moreover, the higher count rates arising from the use of screened tips may also allow spectra to be collected at reduced tip-surface distance, with possibly enhanced spatial resolution.

In summary, we have reported experimental SPELS spectra (of graphite) obtained with a microfabricated coaxial tip. The spectra show the usual π and σ plasmon peaks and, in particular, intense SEE peaks, in comparison, for example, with a simple Au cathode tip. The SEE peaks are assigned to critical points in the unoccupied band structure (i.e., above E_{vac}) of graphite, in generally good agreement with the theoretically calculated band structure. The coaxial tips, which screen the long-range electric field originating from the tip enhance the SEE signal, in general, make visible SEE features arising from the zone edge (M point) as well as zone center (Γ point) in the Brillouin zone, in particular.

The authors thank the EPSRC for financial support. M.Y.S. acknowledges support from the ORS Foundation and the University of Birmingham.

*r.e.palmer@bham.ac.uk

[1] G. Binnig, H. Rohrer, Ch. Gerber, and E. Weibel, Phys. Rev. Lett. **49**, 57 (1982).
[2] B. J. Eves, F. Festy, K. Svensson, and R. E. Palmer, Appl. Phys. Lett. **77**, 4223 (2000).
[3] F. Festy, K. Svensson, P. Laitenberger, and R. E. Palmer, J. Phys. D **34**, 1849 (2001).
[4] R. E. Palmer, B. J. Eves, F. Festy, and K. Svensson, Surf. Sci. **502**, 224 (2002).
[5] R. E. Palmer, Surf. Interface Anal. **34**, 3 (2002).
[6] F. Festy and R. E. Palmer, Appl. Phys. Lett. **85**, 5034 (2004).
[7] J. Yin, A. Pulisciano, and R. E. Palmer, Small **2**, 744 (2006).
[8] A. Pulisciano, S. J. Park, and R. E. Palmer, Appl. Phys. Lett. **93**, 213109 (2008).
[9] J. J. Lawton, A. Pulisciano, and R. E. Palmer, J. Phys.: Condens. Matter **21**, 474206 (2009).
[10] M. Tomitori, H. Terai, and T. Arai, Appl. Surf. Sci. **144**, 123 (1999).
[11] M. Tomitori, M. Hirade, Y. Suganuma, and T. Arai, Surf. Sci. **493**, 49 (2001).
[12] M. Hirade, T. Arai, and M. Tomitori, Jpn. J. Appl. Phys., Part 1 **42**, 4837 (2003).
[13] M. Hirade, T. Arai, and M. Tomitori, Jpn. J. Appl. Phys., Part 1 **45**, 2278 (2006).
[14] X. Zhou, C. Xu, Z. Wei, W. Liu, J. Li, X. Chen, J. F. Williams, and K. Xu, J. Electron Spectrosc. Relat. Phenom. **165**, 15 (2008).
[15] C. Xu, X. Chen, X. Zhou, Z. Wie, W. Liu, J. Li, J. F. Williams, and K. Xu, Rev. Sci. Instrum. **80**, 103705 (2009).
[16] Y. Miyatake, T. Nagamura, K. Hattori, Y. Kanemitsu, and H. Daimon, Jpn. J. Appl. Phys., Part 1 **41**, 4943 (2002).
[17] Y. Miyatake, T. Nagamura, K. Hattori, Y. Kanemitsu, and H. Daimon, Jpn. J. Appl. Phys., Part 1 **42**, 4848 (2003).
[18] S. Mizuno, J. Vac. Sci. Technol. B **19**, 1874 (2001).
[19] S. Mizuno, J. Fukuda, and H. Tochihara, Surf. Sci. **514**, 291 (2002).
[20] S. Mizuno, J. Fukuda, M. Iwanaga, and H. Tochihara, Jpn. J. Appl. Phys., Part 1 **43**, 5501 (2004).
[21] S. Mizuno, F. Rahman, and M. Iwanaga, Jpn. J. Appl. Phys., Part 2 **45**, L178 (2006).
[22] M. Y. Song, A. P. G. Robinson, and R. E. Palmer, Nanotechnology **21**, 155304 (2010).
[23] F. Offi, A. Fondacaro, G. Paolicelli, A. D. Luisa, and G. Stefani, Nucl. Instrum. Methods Phys. Res. A **550**, 454 (2005).
[24] R. C. Tatar and S. Rabii, Phys. Rev. B **25**, 4126 (1982).
[25] N. A. W. Holzwarth, S. G. Louie, and S. Rabii, Phys. Rev. B **26**, 5382 (1982).